# Double-Twisted Helical Lamellar Crystals in a Synthetic Main-Chain Chiral Polyester Similar to Biological Polymers

**Chritopher Y. Li,[†] Donghang Yan,*[,‡] Stephen Z. D. Cheng,*[,†] Feng Bai,[†] Tianbai He,[‡] Lang-Chy Chien,[§] Frank W. Harris,[†] and Bernard Lotz[⊥]**

*Maurice Morton Institute and Department of Polymer Science, The University of Akron, Akron, Ohio 44325-3909; Polymer Physics Laboratory, Changchun Institute of Applied Chemistry, Chinese Academy of Science, Changchun, Jilin 130022, China; Liquid Crystal Institute, Kent State University, Kent, Ohio 44010-0001; and Institute Charles Sadron of Macromolecules, 6 Rue Boussingault, Strasbourg 67083, France*

*Received June 25, 1998*
*Revised Manuscript Received November 30, 1998*

Phase structures, morphologies, and transformation mechanisms of chiral biological and synthetic polymers are fundamentally important topics in understanding their macroscopic responses in different environments. One of the most intriguing findings in the structure and morphology of biological polymers is that *Bombyx mori* silk fibroin can grow a helical lamellar crystal of the $\beta$-modification under solution crystallization conditions.[1] In another example, dinoflagellate chromosomes (in *Prorocentrum micans*) in an in vivo arrangement also displayed the same type of helical structure[2] although it only deals with protein molecular packing in a less ordered form rather than a true crystal as in the case of *Bombyx mori* silk fibroin.

Synthetic polymers having chiral centers along the main-chain backbones are difficult to polymerize, and consequently only a few examples have been reported. This study reports a salient observation of a twisted helical lamellar crystal in one of the first of few chiral main-chain liquid crystalline polyesters. The polymer was synthesized from (*R*)-(−)-4′-{$\omega$-[2-(*p*-hydroxy-*o*-nitrophenyloxy)-1-propyloxy]-1-nonyloxy}-4-biphenyl carboxylic acid. The number of methylene units is nine, and this polymer is abbreviated as PET(R*)-9. The detailed synthetic route will be published elsewhere. In brief, this monomer was synthesized starting from ethyl-(*S*)-(−)-lactate involving Finklstein reaction, alkylation, Baeyer−Villiger oxidation, and Mitsunobu reaction, and then hydrolysis of the corresponding precursor afforded the desired monomer in 11 steps. The polymerization of the chiral polyester was directly prepared from this monomer, hydroxy acid in A−B type, using the catalyst 4-(dimethylamino)pyridinium 4-toluenesulfonate under mild conditions. Its chemical structure is

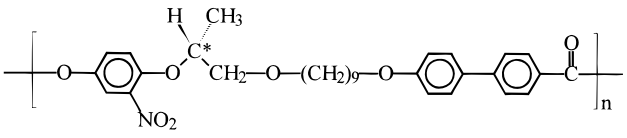


The polymer possesses right-hand chiral centers (*) along the main-chain backbone. The molecular weight of PET(R*)-9 is around 16 000 g/mol, and the polydispersity is approximately 2, as measured by gel permeation chromatography based on polystyrene standards. The chirality of the monomers is $[\alpha]_D = -28.5°$.

Polymer thin films (with a thickness of around 50−100 nm) were prepared via the solution casting method using a 0.05% solution in tetrahydrofuran. After the solvent was evaporated, the films were heated to the isotropic melt. They were subsequently quenched to preset isothermal temperatures and held for various times ranging from several minutes to a few days. The samples were then quenched in liquid nitrogen and allowed to return to room temperature, which is below the glass transition temperature of the polymer ($T_g$ = 37 °C). The thin films were shadowed by Pt and coated with carbon for transmission electron microscopy (TEM) observations (in a JEOL 1200 EX II using an accelerating voltage of 120 kV). Electron diffraction (ED) patterns of the samples were also obtained using a TEM tilting stage in order to determine the three-dimensional crystalline unit cells. Calibration of the ED spacings was carried out using Au and TlCl. To examine the chain folding direction, low molecular weight polyethylene (PE) decoration was utilized following the procedure previously reported.[3,4]

This polymer demonstrated that, upon cooling, a high-temperature chiral smectic liquid crystal phase transition occurs at approximately 189 °C, followed by further ordering processes of crystallization. Figure 1a shows a TEM microphotograph of a flat lamellar crystal grown from the melt at 160 °C for 1 day. The [00*l*] zone ED pattern is shown in Figure 1b. Therefore, this ED pattern represents the *a***b** two-dimensional lattice, and the *b**-axis is parallel to the long axis of the lamellar crystal. The basic unit cell dimensions were determined to be $a$ = 1.07 nm and $b$ = 0.48 nm. The *c*-axis dimension can be determined through the ED patterns of different zones obtained using the tilting stage and was calculated to be 5.96 nm. One can observe that in Figure 1b the (*h*10) layer of this ED pattern is strong. However, there is another parallel diffraction layer (the arrow in Figure 1b) above the (*h*10) layer. The distance between this layer and the (*h*10) layer is one-third of that between the (*h*00) and the (*h*10) layers. The simplest explanation of this observation is that there is a commensurate structure along the *b*-axis which has a spacing 3 times larger than the *b*-dimension of the basic unit. Furthermore, comparing the (*h*10) and (*h*00) layer in the ED pattern (Figure 1b), the diffractions of the (*h*10) layer are 5 times denser than that of the *a** of the basic unit given by the (*h*00) layer diffractions. This may indicate that another commensurate structure also exists and is superimposed on the basic unit cell along the *a*-axis with a periodicity 5 times larger than the *a*-dimension of the unit cell. The cause and nature of these commensurate structures are not clear at this moment, and possible explanations range from a modulated or composite structure to quasi-crystals.

Figure 2a shows a twisted helical lamellar crystal of a PET(R*)-9 sample observed under TEM, which was crystallized at 145 °C for 1 day. In all of our observations, this twisted helix is always left-handed. (Note that the chiral handedness in the chain is right-handed.) The

* To whom correspondence should be addressed.
[†] The University of Akron.
[‡] Chinese Academy of Science.
[§] Kent State University.
[⊥] Institute Charles Sadron of Macromolecules.

10.1021/ma981000a CCC: $18.00 © 1999 American Chemical Society
Published on Web 12/29/1998

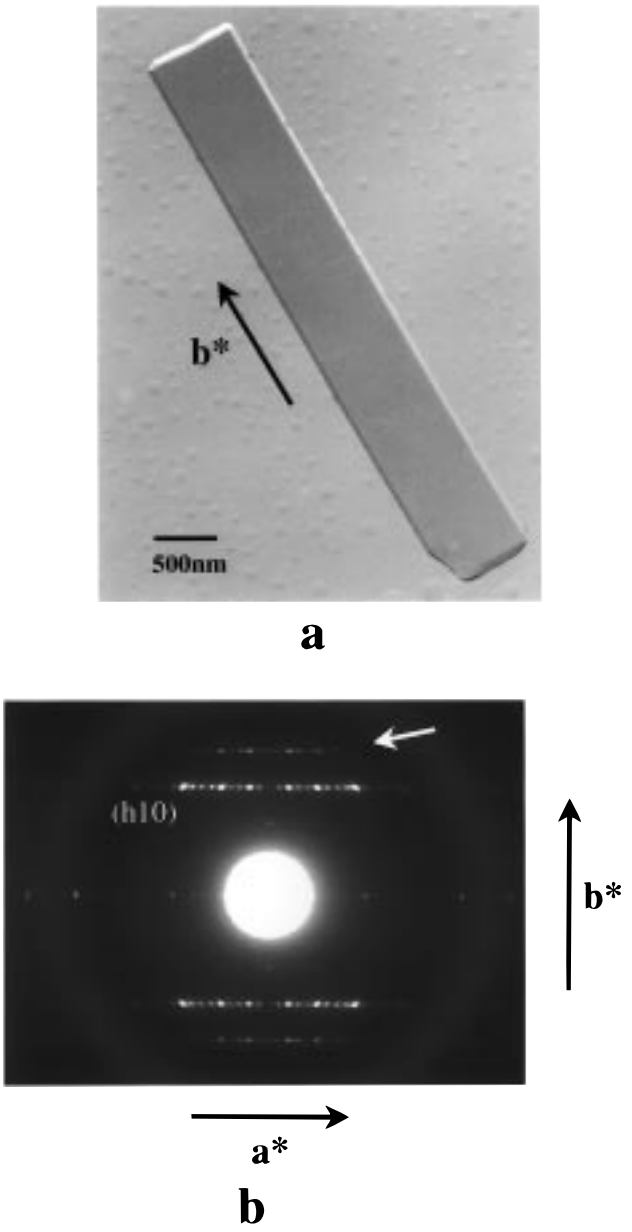


**Figure 1.** A flat lamellar crystal grown from the melt at 160 °C for 24 h and observed under TEM (a) and its corresponding ED pattern (b).

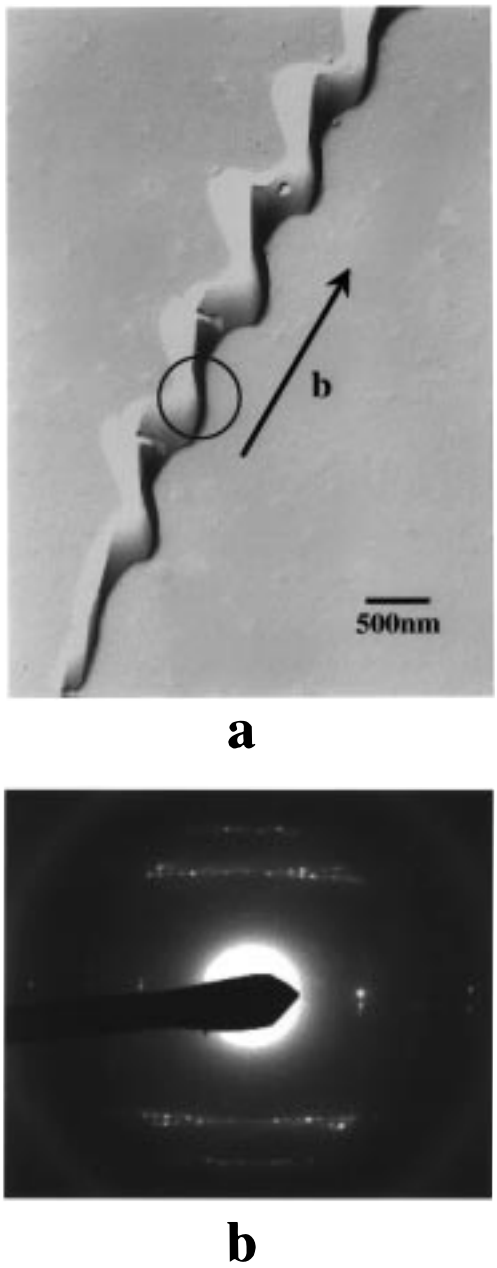


**Figure 2.** A double-twisted helical lamellar crystal grown from the melt at 145 °C for 24 h and observed under TEM (a) and its corresponding ED pattern (b).

pitch length is 2.0 $\mu$m. On the basis of the heavy metal shadowing technique, one can estimate the lamellar thickness to be approximately 15 nm. The crystal surfaces observed at this photograph resolution appear smooth with a continuous and periodically changing curvature. The ED pattern obtained from this helical lamellar crystal is shown in Figure 2b. It is evident that the helical lamellar crystals possess the same crystal structure as the flat single lamellar crystal by comparing Figure 2b with Figure 1b. In the area where the ED is taken, two ED patterns are superimposed with a rotation angle of 6° along the substrate normal. The reciprocal lattice calculation shows that these two ED patterns contain the [13$\bar{1}$] and [36$\bar{2}$] zones, respectively, which indicates that they arise from two different orientations of the single-crystal lattice. It should be noted that within the lattice of the flat crystal the [13$\bar{1}$] and [36$\bar{2}$] zones should be 7.88° apart from each other, while in Figure 2b both zones are aligned with the electron beam direction. The superposition of these two zones in Figure 2b indicates that these two crystal orientations deviate from that in the lattice of the flat crystals, which is characteristic of the twisted crystals. Furthermore, the 6° rotation between these two ED patterns (Figure 2b) implies that there is 6° angle between the intersections of the two $b^*c^*$-planes with the substrate surface. Therefore, the ED pattern in Figure 2b provides experimental evidence that this lamellar crystal is double-twisted. If the helical crystal observed in Figure 2a had a single-twisted helical geometry (such as in the cholesteric phase), the *b*-axis direction would not change.

The concept of double-twisted morphology can be described in Figure 3 wherein only a single center parent sheet with a constant thickness is given. The parent sheet can be built from a continuous helical rotation of elongated units which simultaneously follow a translation along the long axis of the sheet. Many of

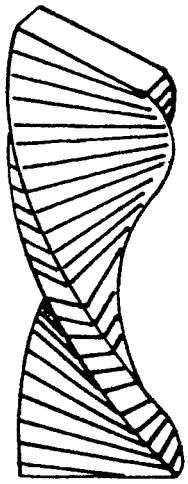

**Figure 3.** Schematic drawings of the double-twisted helical geometry: a stacking of chain molecules to form a double-twisted geometry with a more or less "orthogonal" cross section along the long helical axis. Note that in this drawing the long helical axis is tilted around 30° toward readers in order to view the cross sections.

these helical sheets stack on both sides of the parent sheet. Between the neighboring sheets, another continuous helical rotation exists along an axis that is perpendicular to the long helical axis. One thus obtains a double-twisted geometry.[5] This type of geometry has been observed in biological polymers that involve the twisted $\beta$-pleated sheets,[6−8] such as in the cases of globular proteins wherein several $\beta$-pleated sheets are embedded into a relatively less-ordered environment,[9] *Bombyx mori* silk fibroin helical lamellar crystal of the $\beta$-modification grown from solution,[1] and dinoflagellate chromosomes (in *Prorocentrum micans*) in an in vivo arrangement.[2] It should be noted that most of these structures in biological polymers are in liquid crystalline rather than crystalline states.[10]

It is intriguing that the flat and helical lamellar crystals possess the same crystal structures. Crystallographically, it is impossible to use translation symmetry to transfer a smoothly twisted (curved) lattice into a flat (linear) one in three-dimensional space. Therefore, defects must play a role. This may be viewed as a geometrically frustrated crystal and can be formed in two possible ways. First, the twisted helical crystals may be constructed through a continuous deformation of crystal unit cells due to bending moments (a continuous model). In this case, each molecular layer (the thickness of this layer is half of the *b*-dimension in the basic cell) in the lamellar crystal is deformed to cause a three-dimensional twist. The rotational angle between adjacent layers along the long helical axis can be approximately estimated by calculating the ratio between the pitch length (from 1.5 to 3.0 $\mu$m) and one molecular layer thickness (0.24 nm). This approximation leads to an angle between 0.03° and 0.06° per molecular layer along the long helical axis depending upon the crystallization temperatures.

The second possible way involves the crystal being divided into small, discrete domains with a certain size and within each of these domains the flat crystal structure exists. The boundary between two domains acts as defects (a discrete model). These defect boundaries must be small enough in size in order to maintain a relatively low overall free energy and retain a stable helical crystal. Hence, the overall twisted structure consists of a number of unfrustrated domains connected by dislocation defects.[11,12] This has been observed in less ordered liquid crystalline phases such as the twisted grain boundary phases.[13,14] Based on our observations, the twist surfaces seem to be smooth and continuous down to a size resolution of 10 nm under the TEM observations.

The question pertaining to the mechanism of the double-twisted helical crystals formation of the long chain chiral molecules is also essential to resolve. One must first know whether the chain molecules are folded and, if so, what the folding direction is. The low molecular weight PE decoration method[3,4] was utilized in our experiments. Parts a and b of Figure 4 show the results for the flat and double-twisted helical lamellar crystals, respectively. It is clear that in Figure 4a the elongated direction of the PE decorated crystals is perpendicular to the *b*-axis (the long lamellar axis) of the flat crystals and the *c*-axis of the PE crystals is parallel to the *b*-axis of the crystal. Therefore, the chain folding direction is along the *b*-axis (the long lamellar axis). On the other hand, in Figure 4b, the PE decorated helical crystal shows that the elongated direction of the PE crystals is globally perpendicular to the long helical axis. One can thus conclude that in the helical crystals the chain folding direction is also along the rotated *b*-axis. These observations are similar to the case of $\beta$-pleated sheets in globular proteins and other biological polymers in which the protein folding is along the advancing direction (helical direction) of the sheets. Moreover, in Figure 4b, decorated PE crystal shows that both the top and bottom of the helical crystal surfaces exhibit identical folding behavior.

Upon increasing the isothermal crystallization temperature, the periodicity (pitch length) of the helical lamellar crystals expands from approximately 2.0 $\mu$m at 145 °C to virtually flat at 160 °C. Furthermore, it is also observed that in some cases the flat single lamellar crystal may be converted to the helical crystal and vice versa. This conversion appears to occur on a molecular packing scale, indicating again that the flat crystals may provide an example of suppression of the chirality due to crystallization, while the helical lamellar crystals may represent a geometrically frustrated structure which is caused by the chirality. Detailed analyses will be reported in the near future.

Chiral helical structures are well-known in low ordered liquid crystalline phases, such as in cholesteric, smectic C*, and twisted grain boundary phases. When chiral liquid crystals are able to crystallize (such as in smectic crystal G*, H*, J*, and K* phases), generally speaking, the helical structures that appear in low ordered chiral liquid crystalline phases are suppressed due to the crystallization providing a greater interaction.[15] Another apparently related issue of the twisted lamellar crystals is in the banded spherulitic morphology of synthetic nonchiral polyethylene (PE) and other polymers.[16,17] To explain the banded texture of PE spherulites, it has been found that the chain direction in highly elongated PE single crystals in thin films supported on a substrate is tilted toward the *a*-axis. This leads to different reentrant angles between the lateral growth surface and substrate and therefore anisotropic growth rates along both sides of the (200) directions in the single crystals. The corresponding structural asymmetry in these single crystals causes a significant longitudinal bending moment in the crystals and intro-

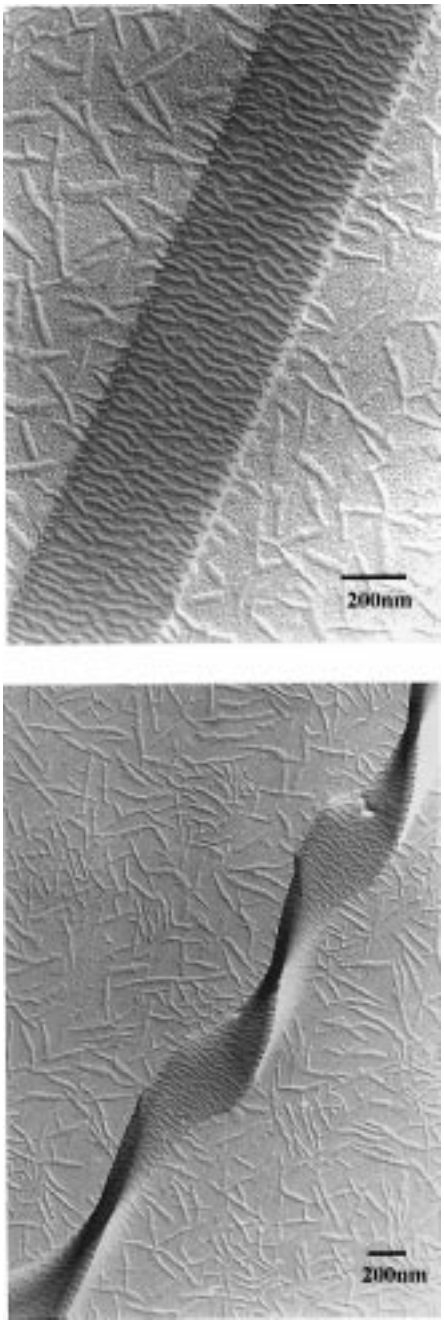


**Figure 4.** Low molecular weight PE crystals decorated PET*-9 flat lamellar crystal (a, top) and double-twisted helical lamellar crystal (b, bottom) observed under TEM. The *c*-axis of the PE crystals (which is perpendicular to the needlelike PE crystals) is parallel to the long axis of both the lamellar crystals. The crystallization conditions are the same as in Figures 1 and 2.

duces the lamellar twisting.[18] Chiral poly(epichlorohydrin)s with both antimorphs have also been found to form banded spherulites, but no tilted single lamellar crystals have been reported.[19,20]

In conclusion, there are at least three novel observations in this study. First, PET(R*)-9 double-twisted lamellae are crystallized from the melt rather than in solution, indicating that this structure is an intrinsic character of the chiral polymer and not a result of solvent interaction. Furthermore, $\beta$-pleated sheets are not present in PET(R*)-9 since no hydrogen bonding exists in this polyester, revealing that the chiral configuration is the only necessary condition for the formation of this helical lamellar crystal. Second, the helical crystals possess a regular orthorhombic unit cell structure, identical to that of the flat lamellar crystals. This observation provides a real opportunity to identify the formation mechanisms of the helical crystals (the continuous versus discrete models). Third, the molecular chain folding is along the *b*-axis in both flat and helical lamellar crystals, indicating that the chain folding is directly toward the less ordered liquid crystalline state. With the exception of the observations of crystallization from the melt, the chiral main-chain polyester has exhibited a remarkable similarity to biological polymers in both phase formation and morphology.

**Acknowledgment.** We thank NSF (DMR-9617030) and NSF STC ALCOM (DMR-8920147) for funding. S.Z.D.C., D.Y., and T.H. also acknowledge the cooperative research grants from Chinese NNSF (29474143 and 29674030). The authors also acknowledge the extensive discussions with Dr. F. A. Khoury at National Institute of Standard and Technology and Professor A. Keller at University of Bristol.

## References and Notes

(1) Lotz, B.; Gonthier-Vassal, A.; Brack, A.; Magoshi, J. *J. Mol. Biol.* **1982**. *156*, 345.
(2) Livolant, F.; Bouligand, Y. *Chromosoma* **1980**, *80*, 97.
(3) Wittmann, J. C.; Lotz, B. *Makromol. Rapid Commun.* **1982**, *3*, 733.
(4) Wittmann, J. C.; Lotz, B. *J. Polym. Sci., Polym. Phys. Ed.* **1985**, *23*, 205.
(5) Kleman, M. *Rep. Prog. Phys.* **1989**, *52*, 555.
(6) Marsh, R. E.; Corey, R. B.; Pauling, L. *Biochim. Biophys. Acta* **1955**, *16*, 1.
(7) Lucas, F.; Shaw, J. T. B.; Smith, S. G. *Biochem. J.* **1957**, *66*, 468.
(8) Chothia, C. *J. Mol. Biol.* **1973**, *75*, 295.
(9) Chothia, C.; Levitt, M.; Richardson, D. *Proc. Natl. Acad. Sci. U.S.A.* **1977**, *74*, 4130.
(10) Livolant, F.; Leforestier, A. *Prog. Polym. Sci.* **1996**, *21*, 1115.
(11) Kleman, M. *Adv. Phys.* **1989**, *38*, 605.
(12) Kamien, R. D.; Nelson, D. R. *Phys. Rev. E* **1996**, *53*, 650.
(13) Renn, S. R.; Lubensky, T. C. *Phys. Rev. A* **1988**, *38*, 2132. See also: *Phys. Rev. A* **1990**, *51*, 4392.
(14) Goodby, J. W.; Waugh, M. A.; Stein, S. M.; Chin, E.; Pindak, R.; Patel, J. S. *Nature* **1989**, *337*, 449.
(15) Goodby, J. W.; Slaney, A. J.; Booth, C. J.; Nishiyama, I.; Vuijk, J. D.; Styring, P.; Toyne, K. J. *Mol. Cryst. Liq. Cryst.* **1994**, *243*, 231.
(16) For a recent summary, see: Keith, H. D.; Padden Jr., F. *Macromolecules* **1996**, *29*, 7776.
(17) Briber, R. M.; Khoury, F. A. *J. Polym. Sci., Polym. Phys. Ed.* **1993**, *31*, 1253.
(18) Keith, H. D.; Padden Jr., F.; Lotz, B.; Wittmann, J. C. *Macromolecules* **1989**, *22*, 2230.
(19) Singfield, K. L.; Brown, G. R. *Macromolecules* **1995**, *28*, 8006.
(20) Singfield, K. L.; Hobbs, J. K.; Keller, A. *J. Cryst. Growth* **1998**, *183*, 683.

MA981000A